DETECTION OF LONG PERIOD WAVES IN THE POLAR CORONAL HOLES

D. Banerjee[(1)], E. O'Shea[(2)], J.G. Doyle[(2)], and S. Poedts[(3)]

[(1)]*Indian Institute of Astrophysics, Koramangala, Bangalore 560034, India*
[(2)]*Armagh Observatory, College Hill, Armagh BT61 9DG, N. Ireland*
[(3)]*Center for Plasma Astrophysics, KULeuven, Leuven, 3001, Belgium*

ABSTRACT

We examine long spectral time series of polar coronal holes with the Coronal Diagnostic Spectrometer (CDS) on-board SoHO. Previously, the presence of long period waves in the plumes and inter-plume regions has been reported from the observations of transition region lines. From the current study of several coronal lines we will report on the presence of long period outwardly propagating slow magneto-acoustic waves in several locations. We will also try to search for the origin of these waves and will report on the connection, if any, of network boundaries in the disk part of the coronal holes and the plume and inter-plumes. These slow magneto-acoustic waves may contribute significantly to the heating of the lower corona by compressive dissipation and may also provide some of the energy flux required for the acceleration of the fast solar wind.

Key words: Sun: Corona: Oscillations: coronal hole: Waves.

1. INTRODUCTION

When viewed off-limb, polar plumes are the most prominent structures in polar coronal holes (DeForest et al. 1997; Koutchmy & Bocchialini 1998). More recently, DeForest et al. (2001) produced images from LASCO/SoHO, which clearly show polar plumes extending to altitudes of 30 solar radii or more, very close to the outer edge of the C-3 field of view and above the likely Alfv́enic point of the wind flow. Plumes are considered to be bright threads rooted in the network and are thought to form at the network boundaries where small bipoles within a coronal hole reconnect with unipolar flux concentrations (Wang & Sheely 1995; Wang 1998). It has been known that the density of the plumes are much higher (3-5 times) than the inter-plume background (Saito 1965; Ahmed & Withbroe 1977; Young et al. 1999) implying that the coronal heating rate is not uniform over the coronal hole. Plume formation involves magnetic reconnection between unipolar flux concentrations and nearby bipoles, but the bipolar fields constitute only a small fraction of the total magnetic flux within the polar coronal hole. Primarily, coronal holes are overwhelmingly unipolar. This fact further suggests that plumes are not the source of the high speed polar wind (Wang et al. 1997), but probably the inter-plumes are. Banerjee et al. (2000) investigated the temporal behaviour of polar plumes as observed in the transition region line, O v 629Å. In this paper we report on the temporal behaviour of the plume and inter-plume lanes as observed by the CDS/SoHO instrument but extending the previous studies which were restricted to transition region temperatures to coronal heights.

Table 1. A log of the datasets.

Date	Dataset	Pointing (X,Y)	Region	Start time
29/11/02	26348	116,1085	plume	18:42
02/12/02	26363	54,1070	plume	07:50
06/12/02	26406	-1,1070	plume	07:00
11/12/02	26438	-19,1070	plume	16:29
12/12/02	26447	56,1070	plume	16:30
13/12/02	26452	-29,1071	Int-plume	12:10
17/12/02	26478	59,1071	plume	18:03
18/12/02	26482	-1,-1076	Int-plume	06:58
27/12/02	26542	0,1070	plume	18:10
31/12/02	26568	-1,1070	plume	11:58

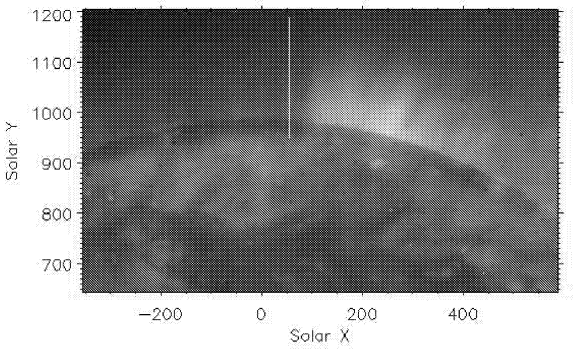

Figure 1. Location of the slit for the 2nd December 2002, s26263, dataset.

2. OBSERVATIONS AND DATA REDUCTION

For these observations we have used the normal incidence spectrometer (NIS) (Harrison et al. 1995), which is one of the components of the Coronal Diagnostic Spectrometer (CDS) on-board the Solar and Heliospheric Observatory (SOHO). The details of the observations including pointing and start times are summarised in Table 1. The temporal series sequence SER150W was run and data ob-

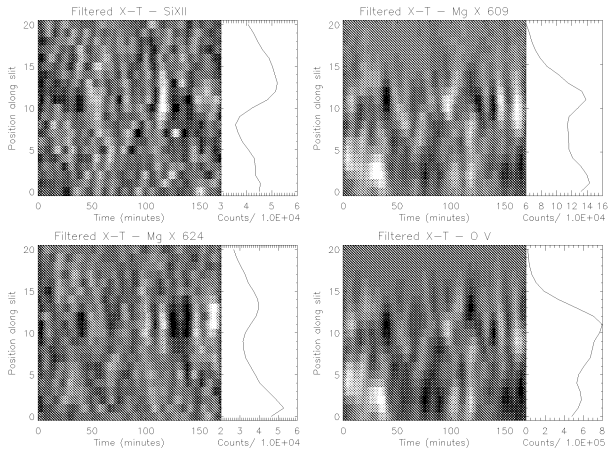

Figure 2. Space time behaviour of different temerature lines (X-T slice), for dataset s26363, plume.

tained for 11 transition region and coronal lines formed between 2.5×10^5 K and 2.5×10^6 K.

In this paper, however, we shall only make use of the most useful of these, the transition region O V 629 Å line ($\sim 2.5 \times 10^5$ K) and the coronal lines of Mg X 609, Mg X 625 Å ($\sim 1 \times 10^6$ K) and Si XII 520 Å ($\sim 2.5 \times 10^6$ K). All the data were obtained with the 4 × 240 arcsec slit with exposure times of 60 sec., corresponding to 150 time frames. In order to increase the signal-to-noise ratio we binned by 2 along the slit to produce 70 pixels in Y. The line profiles were then each fitted with a single Gaussian in order to measure the intensity and the line-of-sight (LOS) velocity. We note that the bakeout that CDS suffered during the SOHO loss in 1998 changed the line profiles produced by the NIS spectrometer.

The NIS1 profiles exhibit broader wings and the NIS2 profiles show a broadened and asymmetrical long wavelength wing. The fitting of the lines takes these broadened and asymmetric lines into account by using the BGAUSS option of the CFIT Gaussian fitting routines available in the CDS software tree in SOLARSOFT. Since we are always looking at the polar regions in these observations the rotation of the Sun should not move our observing region significantly over the duration of the observations despite the fact that the observations were obtained in a sit-and-stare mode, i.e. no rotational compensation was used.

The data was first cleaned of cosmic ray hits by using the CDS software procedures CDS_CLEAN and CDS_NEW_SPIKE. Using the standard CDS software procedure VDS_CALIB the data was then de-biased and flat fielded. Other effects such as fixed pattern effects and CCD burn-in were also corrected for with this procedure. Slant and tilt corrections were applied to the data using another CDS software procedure, NIS_ROTATE. As we are solely using data from NIS2 in this work it was not necessary to 'switch on' the /ALIGN keyword in this NIS_ROTATE routine to account for the spatial offset typically present between NIS1 and NIS2. Further and fuller details on cleaning and calibrating CDS data may be found at http://solg2.bnsc.rl.ac.uk/software/uguide/uguide.shtml.

The resulting data after carrying out the reduction of the data are in units of photon-events/pixel/sec. Multiplying by the exposure time yielded units of photon-events/pixel which were those used in this work. The total number of photon-events in a line was obtained by integrating under the fitted line profile. The velocity values presented in this paper are relative velocities, that is, they are calculated relative to an averaged profile, obtained using the limb method, i.e. the summed profile at the limb whose averaged LOS velocity is assumed to be zero. This averaged profile was fitted by a Gaussian and its 'rest' wavelength determined. All other profiles were then measured relative to this 'rest' wavelength and the resulting 'velocities' estimated. No absolute calibration exists for the velocity scale, so that the derived velocities are therefore merely indicative of the presence of line shifts.

3. RESULTS

3.1 Plume oscillations

In Fig. 1 we show the location of the slit for one representative dataset, s26363, as observed on 2nd december. The pointing of the slit was positioned at the north polar limb in such a way that a major part of the slit was outside the limb and a part on the coronal hole. The background image is taken from EIT 195 Å a few hours before our observations.

First we concentrate on dataset s26363. In Fig. 2) We show the space time behaviour (in a portion of the slit which focuses on the plume region and the coronal hole) as observed by different temperature lines, in the form of X-T slices (the grey scale panels). To bring out the details of the original intensity map (X-T slice) we have filtered out the high frequency components in the image (see Doyle et al. 1999 for details).

In this contrast enhanced image, the solar north-south (SOLAR_Y) direction is in the vertical axis, the horizontal axis is time. The right panels show the total number of counts in a pixel. The grey scale coding has the most intense regions as white. The alternate bright and dark ridges indicate the presence of oscilations in intensity.

Now we present in Fig 3 the wavelet results for intensity and Fig 4 for velocity in different temperature lines, corresponding to a single pixel (px 13) within the plume as recorded in the s26363 dataset. We should point out here that the velocity signal is often weak for the coronal lines in a single pixel and the resulting oscillations are most of the time not significant. Thus we do not show plots for velocity power in this short contribution. The intensity variations are shown in the top panels. In the wavelet spectrum the dark contour regions show the locations of the highest power. The light white horizontal

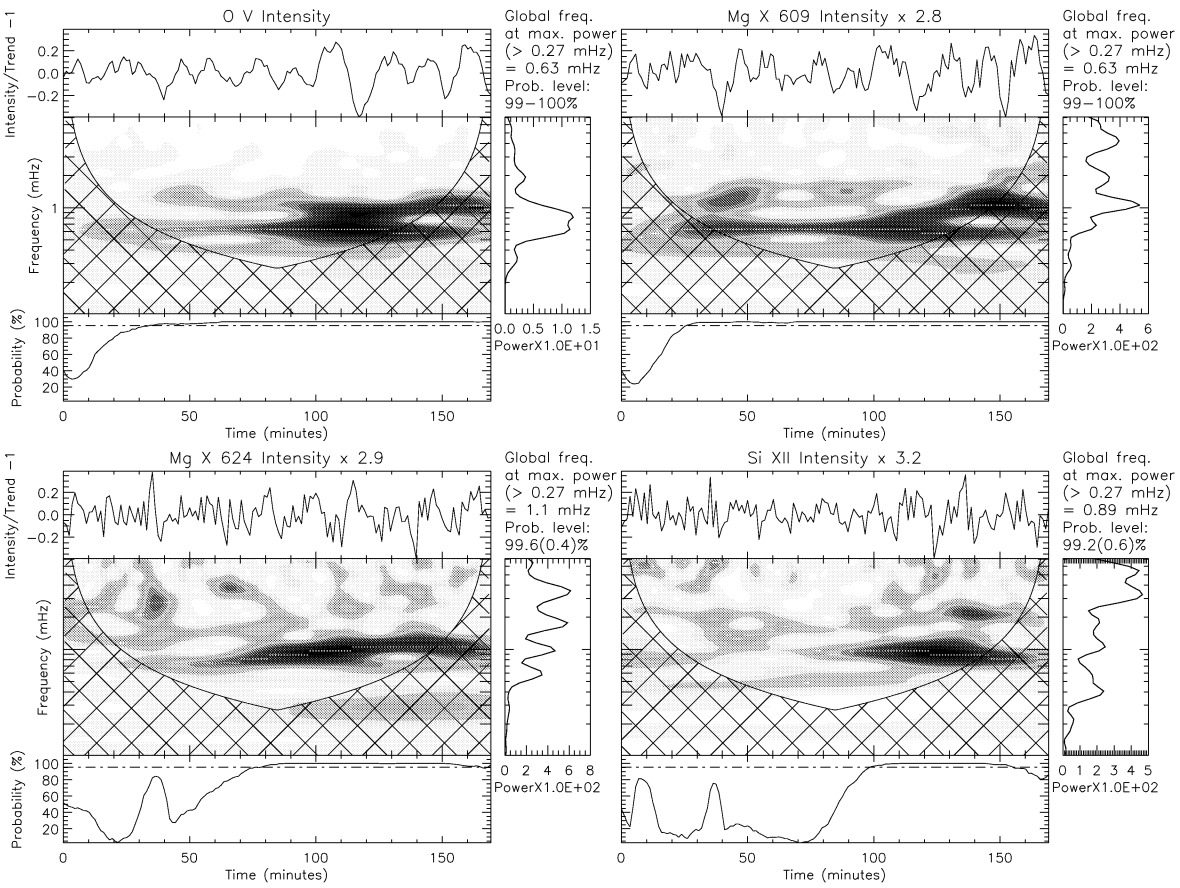

Figure 3. Intensity wavelet results for pixel location 13, within a plume, corresponding to the dataset s26363.

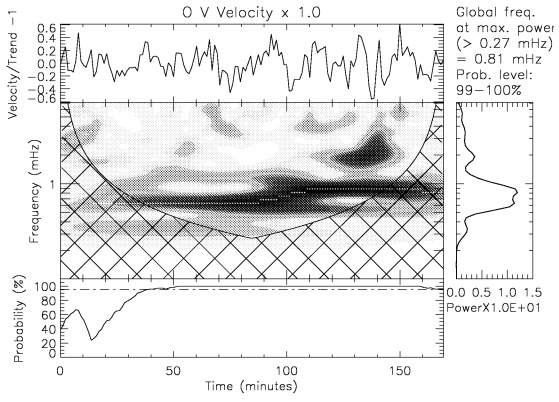

Figure 4. Velocity oscillations corresponding to the s26363 dataset, in the plume and for the O V line.

lines within the dark contour regions indicate the locations of the maximum wavelet power at each particular time. The lowest panel shows the variation of the probability level over the observing time, by which it is possible to see whether the maximum wavelet power at any time in the wavelet spectrum has a high or low probability of being due to noise. Only locations that have a probability greater than 95% are regarded as being real, *i.e.* not due to noise. Cross-hatched regions, on either side of the wavelet spectrum, indicate the 'cone of influence' (COI), where edge effects become important (see Torrence & Compo, 1998).

Next, we show the spatial behaviour of the oscillation frequencies measured from the different temperature lines in Fig. 5. These figures show the measured frequencies as a function of position along the slit (X-f slice). The circles and the plus symbols correspond to the primary maxima and the secondary maxima in the global wavelet power spectra, which have a probability of more than the 95% after the randomisation test. The total number of counts in a pixel (summed counts) during the observation is shown in the right column, and is useful in identifying the limb (pixel 11 corresponds to the limb). It also shows the intensity fall off as we go outside the limb (pixel 11

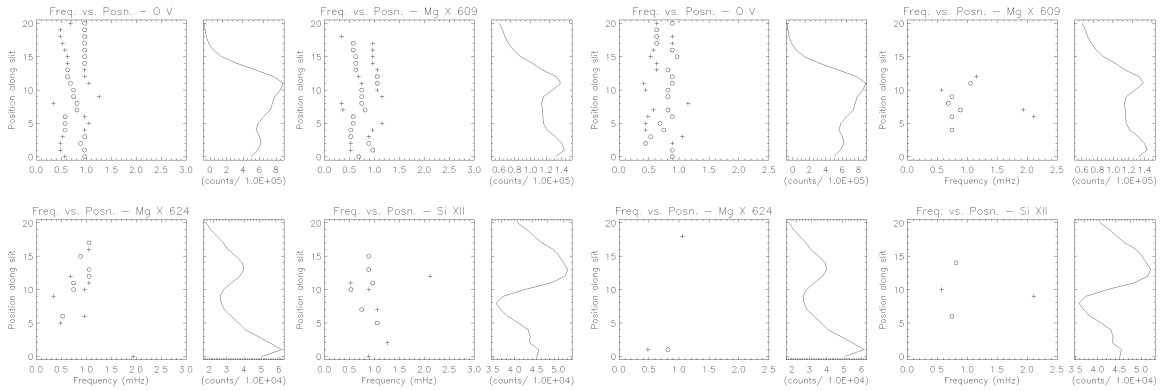

Figure 5. For dataset s26363, plume, spatial variation of frequency corresponding to different temerature lines, X-f slices for intensity (the group of four panels in the left) and for the velocity (group of four panels on the right).

and lower). The intensity and velocity results both show that the primary maxima in the global wavelet spectra lies in the range 0.5-1.0 mHz. The appearance of more points in the intensity X-f slices as compared to the velocity also indicates that the intensity oscillations are stronger and more reliable ($> 95\%$ probability level). Furthermore, it is interesting to note that these low frequency oscillations are also present on the disk part (very close to the limb, e.g. from pxs 0–11), just below the plume. This gives an indication that whatever is causing these oscillations in the plumes is also present on the bright part of the disk.

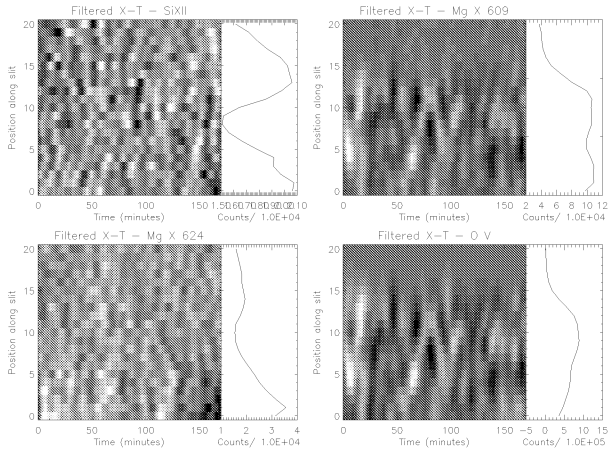

Figure 6. Space time behaviour of different temerature lines (X-T slice), for dataset s26452, inter-plume.

3.2 Inter-plume oscillations

Now, we turn our attention to a dataset s26452, which was taken within an inter-plume lane (see Table 1). As before we show the X-T slices (grey scale panels of Fig. 6) corresponding to diffrent temperature lines. The alternate bright and dark ridges again indicate the presence of oscillations. We look at the same pixel location within the inter-plume (as in the previous case of the plume, pixel 13) and plot the wavelet results in Fig 7. The transition region line O V and the other coronal lines, all show significant oscillations within 0.7-0.9 mHz. Finally in Fig. 8, we plot the spatial variation of the frequency distribution for the same part of the slit as in Fig. 5. Once again it shows the presence of the same frequency dominance across many locations.

4. DISCUSSION

High-cadence EIT/SoHO observations indicate that quasi periodic fluctuations with periods of 10-15 minutes are present in polar plumes (DeForest & Gurman 1998), with a filamentary structure within the plume, on a spatial scale of 3-5 arc sec. These authors conclude that the waves are either sound waves or slow magneto-acoustic waves, propagating along the plumes at $\sim$ 75–150 km s^{-1}. Ofman et al. (2000a) detected quasi periodic variations in the polarization brightness (pB) at 1.9 $R_{\odot}$, in both plume and inter-plume regions. Their Fourier power spectrum shows significant peaks around 1.6-2.5 mHz and additional smaller peaks at longer and shorter timescales. Their wavelet analysis of the pB time series shows that the coherence time of the fluctuations is about 30 minutes.

It is likely that the waves detected at 1.9 $R_{\odot}$ by Ofman et al. (1997, 2000a,b) using UVCS/SoHO and the waves detected by DeForest & Gurman (1998) around 1.2 $R_{\odot}$ using EIT/SoHO are the same as those reported here and as also observed in transition region lines by CDS/SoHO in the polar plumes, very close to the solar limb and in the network boundary of the coronal holes by Banerjee et al. (2000). In this work we have extended the earlier work of Banerjee et al. (2000) to include the coronal lines. The present analysis confirms the presence of these long period oscillations even in the high corona. Thus it is interesting to note that these long period slow waves are present all the way from the chromosphere, through the transition region to the corona. We should also point out

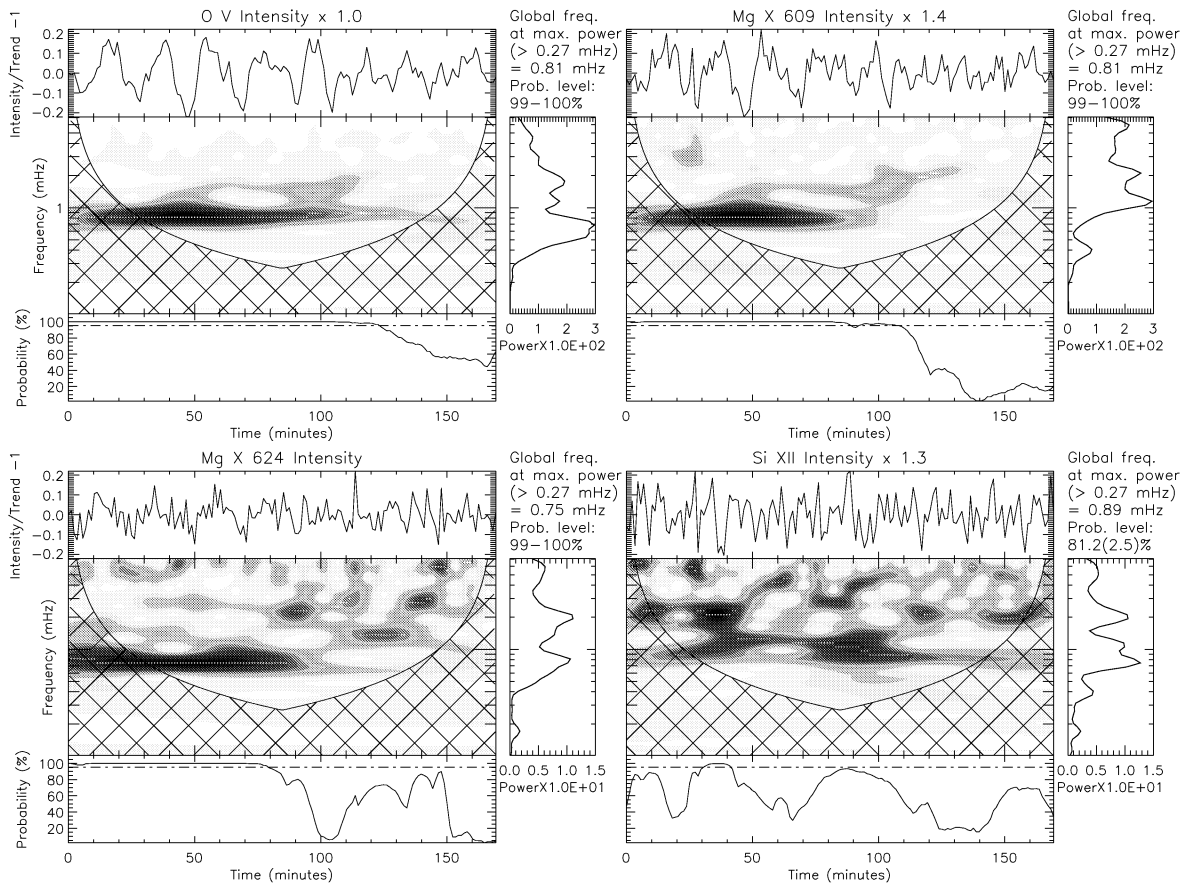

Figure 7. Intensity wavelet results for pixel location 13, within an inter-plume, corresponding to the dataset s26452.

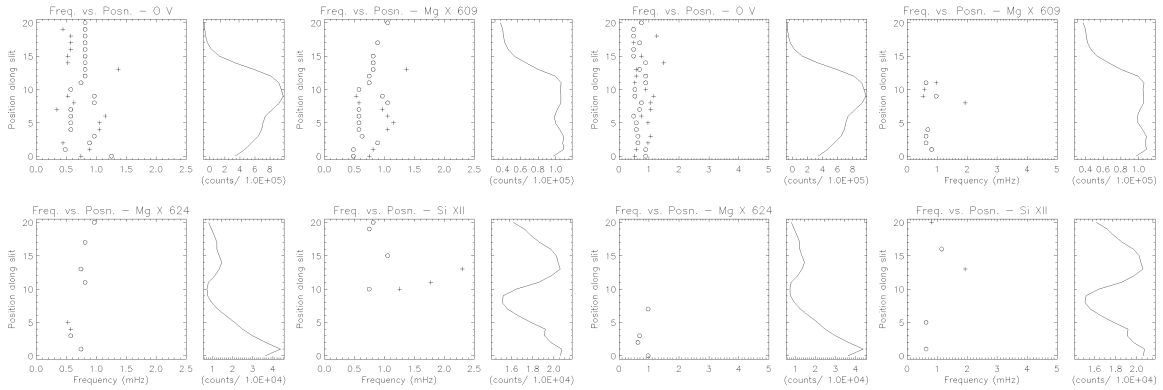

Figure 8. Same as Fig. 5 but for dataset s26452 and in the inter-plume.

that we are detecting similar types of waves (compressional and with long periodicities) in plumes and inter-plume regions close to the limb and also in the disk part of the coronal hole. Ofman et al. (2000a) have also observed these long period waves in plumes and inter-plumes at 1.9 $R_{\odot}$. The periodicity in the inter-plumes seems to be slightly longer than in the plumes. Linear slow magneto-acoustic waves propagate at a speed close to the sound speed in a low β coronal plasma. The long periodicity in the inter-plume may be just a temperature effect on the slow waves; plumes are cooler than the background plasma (DeForest et al. 1997). However, we should also

point out that, because of the line of sight effects and the proximity of the polar plumes to our slit locations, we can not rule out contributions from both regions being present. Another possibility is that the waves detected adjacent to a plume structure could simply be waves which just leaked out of the plume cavity and are propagating through the inter-plume. The details of the present study will be presented in Banerjee et al. (2005).

ACKNOWLEDGEMENTS

We would like to thank the CDS and EIT teams at Goddard Space Flight Center for their help in obtaining the present data and Carl Foley for his help with the GIS data. CDS and EIT are part of SoHO, the Solar and Heliospheric Observatory, which is a mission of international cooperation between ESA and NASA. DB wishes to thank the Royal Society London and the DST, India. His visit to the Armagh Observatory was supported within the India-UK Science Networks program. Research at Armagh Observatory is grant-aided by the N. Ireland Dept. of Culture, Arts and Leisure. This work was supported by a PRTLI research grant for Grid-enabled Computational Physics of Natural Phenomena (Cosmogrid). The original wavelet software was provided by C. Torrence and G. Compo, and is available at URL: http://paos.colorado.edu/research/wavelets/.

REFERENCES

Ahmad, I. A., Withbroe, G. L., 1977, Sol. Phys., 53, 397

Banerjee, D., O'Shea, E. , & Doyle, J.G. 2000, Sol. Phys., 196, 63

Banerjee, D., O'Shea, E. , Doyle, J.G. & Poedts, S., 2005, A&A (to be submitted)

De Forest, C.E., Hoeksema, J.T., Gurman, J.B.,et al. , 1997, sol. phys, 175, 393

DeForest, C.E., & Gurman, J.B. 1998, ApJ, 501, L217

De Forest, C.E., Plunkett, S.P., Andrews, M.D.,et al. , 2001, ApJ, 546, 569

Doyle, J.G., van den Oord, G.H.J., O'Shea, E., Banerjee, D. 1999, A&A, 347, 335

Harrison, R.A., Sawyer, E.C., Carter, M.K., Cruise, A.M. et al., 1995, sol. phys, 162, 233

Koutchmy, S., Bocchialini, K., 1998, ESA SP-421, ISBN: 9290926848, p.51

Ofman, L., Romali, M., Poletto, G., Noci, G., & Kohl, J.L. 1997, ApJ, 491, L111

Ofman, L., Romali, M., Poletto, G., Noci, G., & Kohl, J.L. 2000a, ApJ, 529, 592

Ofman, L., Nakariakov, V.M., & Selegals, N. 2000b, ApJ, 533, 1071

Saito, K., 1965, PASJ, 17, 421

Wang, Y.-M., Sheeley,N.R., Jr., 1995, ApJ, 452, 457

Wang, Y.-M., et al. 1997, ApJ, 484, L75

Wang, Y.-M., 1998, ApJ, 501, L145

Young, P.R., Klimchuk, J.A., Mason, H.E., A&A, 1999, 350, 296